"Rationally Designed Flame-Retardant Coating by Vapor Polymerization for Obtaining Lyocell Blended Textiles with Multifunctional Properties"

ASS. Prof./ Rehab Taha Hussein Shredah
Assistant Professor of Garments and Textile, Department of Home Economics, Faculty of Specific Education, Alexandria University

D. Emad Sobhy Mohamed Goda
Research doctor, Gas Analysis and Fire Safety Laboratory, Chemistry Division, National Institute for Standards, Giza, Egypt

D. Heba Mohammed Abdallah
Polymers and Pigments Department, Chemical Industries Research institute, National Research Center, Dokki, Giza, Egypt

ASS. Prof. / Heba Gamal Abdelhaleem Elsayed
Assistant Professor of Garments and Textile, Department of Home Economics, Faculty of Specific Education, Alexandria University

Abstract:

Pyrrole Vapor Polymerization (PVP) is a green, easy, and advantageous approach to attach improved multilateral features to various substrates for being implemented in different aspects.

The research aims to study the possibility of to rationally designed flame-retardant coating by vapor polymerization for obtaining lyocell blended textiles with multifunctional properties.

In this study, a newly straightforward PVP was stimulated on Lyocell blend textiles using both $AgNO_3$ and $KMnO_4$ as oxidants that were formerly dissolved in CMC polymer. The mass ratios between the two oxidants were altered to yield new composite textiles.

When a redox interaction occurred between pyrrole vapor and MnO_4/Ag anions, a new silver and manganese dioxide@Polypyrrole (Ag-MnO_2@Ppy) was formed as an effective coating for obtaining smart multifunctional textiles.

The structural, morphological, thermal, and mechanical features of as-developed fabrics were investigated. Notably, MnO_2 and Ag nanoparticles were grown inside polypyrrole nano granules on textile with size diameters of ~583, and 58 nm, respectively.

In addition, the UV protection, conductivity, antimicrobial activity, and fire safety properties were studied. The electrical resistance of the composite modified textiles was estimated as(26.3 MΩ) , which is relatively lower than the pure Lyocell fabric (165 MΩ). A highly improved ultraviolet protection factor was recorded also for the coated textile (33.69) compared to the pure one (6.2). Also, the textile composites could retard the microbial infection with measured inhibition zone diameters of 29, and 28 mm for E. coli, and S. aureus, respectively approving an excellent antimicrobial manner. Moreover, the flammability tests stated that the rate of burning of coated textile was measured to be 0 mm/min with regard to the virgin Lyocell fabric (172.5 mm/min). In addition, the afterflame, and glow times were noted as 0, and 395 sec compared to 14, and 35 sec for the uncoated textiles assuring an efficient retardation performance against flame spread.

Keywords:

Lyocell textiles, pyrrole vapor polymerization, Ag-MnO_2@Polypyrrole, flame retardant, antibacterial, UV protection, conductivity.

" تصميم طلاء مبتكر مقاوم للهب باستخدام البلمرة بالبخار للحصول على خواص متعددة الوظائف لمنسوجات الليوسيل المخلوطة "

ملخص البحث :

تعد عملية بلمرة بخار البيرول (PVP) طريقة صديقة للبيئة وبسيطة ومفيدة لربط ميزات متعددة الأطراف محسنة بمختلف الركائز ليتم تنفيذها في جوانب مختلفة.

يهدف البحث لدراسة إمكانية تصميم طلاء مبتكر باستخدام البلمرة بالبخار للحصول على خواص متعددة الوظائف لمنسوجات الليوسيل المخلوطة.

تم تحفيز عملية بلمرة بخار البيرول الجديدة والمباشرة على منسوجات الليوسيل المخلوطة تحت البحث باستخدام كل من نترات الفضة وبرمنجنات البوتاسيوم كمؤكسدات مذابة سابقاً في بوليمر كربوكسي ميثيل كيتوزان، بالاضافة لتغيير النسب بين المؤكسدات لإنتاج منسوجات مركبة جديدة، وعند حدوث تفاعل الأكسدة والاختزال بين بخار البيرول وأنيونات متراكب أكسيد المنجنيز مع الفضة النانونية، تم تشكيل متراكب من أكسيد المنجنيز مع الفضة النانوية والبولي بيرول كطلاء فعال للحصول على منسوجات ذات خواص ذكية متعددة الوظائف.

تبع ذلك إجراء مجموعة من الاختبارات المعملية للتحقق من الخصائص البنائية والشكلية والحرارية والميكانيكية للأقمشة المطورة، والجدير بالذكر أن أكسيد المنجنيز والفضة النانونية نمت داخل حبيبات نانونية من البولي بيرول على المنسوجات بأقطار حجمية تبلغ (٥٨٣، ٥٨) نانومتر على التوالي، بالإضافة إلى ذلك تم دراسة خواص مقاومة الأشعة فوق البنفسجية والتوصيل الكهربائي، مقاومة الميكروبات، مقاومة اللهب"الاشتعال"، تم تقدير المقاومة الكهربائية للمنسوجات المعدلة المركبة بـ (٢٦.٣ MΩ) ، وهي أقل نسبياً من نسيج الليوسيل غير المعالج حيث بلغت قيمته (١٦٥MΩ)، كما سجلت مقاومة الأشعة فوق البنفسجية، تحسن مرتفع للغايه للنسيج المعالج حيث بلغ قيمته (٣٣.٦٩) مقارنةً بالنسيج غير المعالج بلغ (٦.٢)، كما ثبت أن النسيج المعالج يمكن أن يؤخر العدوى الميكروبية بأقطار منطقة

تثبيط تبلغ (٢٩، ٢٨) مم لـ S. aureus ، E. coli على التوالي، مما يؤكد أن مقاومة الميكروبات للمنسوجات تحت البحث ممتاز، علاوة على ذلك أظهرت اختبارات قابلية الاشتعال أن معدل احتراق النسيج المعالج تم قياسه ليكون (٠) مم/ دقيقة وفيما يتعلق بالنسيج غير المعالج فقد بلغ (١٧٢.٥) مم / دقيقة، بالإضافة إلى ذلك تم تسجيل زمن اللهب اللاحق والتوهج على أنها(٠، ٣٩٥) ثانية مقارنة بـ (١٤ ،٣٥) ثانية للمنسوجات غير المعالجة مما يضمن أداء تثبيط فعال ضد انتشار اللهب.

الكلمات المفتاحية :

منسوجات الليوسيل، بلمرة بخار البيرول، متراكب من أكسيد المنجنيز مع الفضة النانوية والبولي بيرول، مقاومة اللهب، مقاومة الميكروبات، مقاومة الاشعة فوق البنفسجية، والتوصيل الكهربائي.

1. Introduction:

The composition of Lyocell blended textiles is mainly made from cellulosic chains and can be used for furnishing, clothing, and many industrial aspects. In general, these fibers possess various important features such as biodegradability, breathability, and comfort [1, 2]. Regrettably, their carbon structure makes them highly flammable, in addition to the warmth retention and high hygroscopicity stimulating the growth of several microbes, which shows unwanted hazards to human life [3, 4]. To solve that, a variety of nitrogen, and phosphorus-based compounds was coated on the textile surface for retarding the flame growth. Also, smart antibacterial materials have to be attached to lyocell blends to inhibit greatly microbial infections for medical applications [4, 5].

To design these coatings on textile surfaces, different approaches have been widely introduced such as layer-by-layer, electrodeposition, and electrospinning [5-7]. However, such techniques owe diverse advantages and shortages, which cannot be easily governed when being implemented in a specific application. Due to high adhesion to the textile surface, easy processing, reproducibility, and availability on a large scale, the dip-coating approach is counted as a promising way to yield an advanced textile [8-10]. Furthermore, various nanomaterials such as manganese dioxide and silver nanoparticles can be exploited as smart coatings to impart improved flame retardancy, mechanical, antibacterial, and conductive behaviors for textiles [8, 11-13]. Nevertheless, the dispersion of these nanoparticles in a polymer matrix is essential before applying them to the textile for harvesting suburb properties and preventing the common instability problem that is observed after the washing process.

Carboxymethyl chitosan (CMC) is counted as a unique polycationic polymer with dual antimicrobial and flame retardancy properties, which is exceedingly implemented in the biomedical industry [8].

Recently, different polymer nanostructures particularly conducting polymers were exploited for stabilizing silver nanoparticles and hence getting new hybrids with multifunctional properties to engineer flexible electronics [14-16]. Various strategies have been proposed for fabricating polypyrrole-silver composite such as electrodeposition, ultrasonic, and UV-assisted polymerization techniques. However, these approaches are complicate and costive.

To the best of our knowledge, multifunctional Lyocell-based fabrics were primarily developed using a prompt, green, and one-step vapor polymerization approach. This is done through the direct exposure of textile impregnated by silver nitrate, $KMnO_4$ oxidants, and CMC to the pyrrole vapor for obtaining a new coating layer from silver and manganese dioxide-decorated polypyrrole composite. Polypyrrole and CMC play a fundamental role in stabilizing Ag, and MnO_2 NPs on the textile surface to overcome their instability issue found after the durability test. The structural, morphological, thermal, and mechanical features of as-developed fabrics were investigated. In addition, the UV protection, conductivity, antimicrobial activity, and fire safety properties were estimated.

2. Experimental:

2.1. Materials:

Lyocell blend textiles are made from fibranne and lyocell (FLC, 50:50) by Masr-Halwan Company, Egypt. $AgNO_3$, Pyrrole, and $KMnO_4$ were supplied from Oxford Laboratory, India. Staphylococcus aureus (S. aureus, RCMB 010028) as a Gram-positive bacterium and Escherichia coli (E. coli, RCMB 010052) as a Gram-negative bacterium were provided by the Regional Center for Mycology and Biotechnology Azhar University-Egypt.

2.2. Preparation of O-carboxymethyl chitosan:

A former report was implemented for synthesizing O-carboxymethyl chitosan (CMC) from the raw chitosan powder. In brief, 1 g of pure chitosan was placed in a round bottom flask containing 20 ml of an equal mixture of isopropanol and NaOH with a concentration of 3.5 M followed by stirring at 30 °C for 1h. To the former solution, a typical mass of 1.5 g measured from mono-chloroacetic acid was progressively added and also stirred for 4 h at a temperature of 55 °C. By using absolute ethanol, the as-obtained suspension was precipitated, and filtered. To also remove the salt, the precipitate was further purified three times by diluted ethanol (70%) and followed by drying in a vacuum oven until it yielded a constant mass. To neutralize the as-gotten product, CMC was re-dissolved in 70% ethanol and subsequent by placing diluted HCl for 30 min. Drying of the formed precipitate is done for 48 h at 30 °C.

2.3. Green engineering of Ag@MnO2-polypyrrole coated FLC textiles:

A new one-pot vapor polymerization approach was utilized to decorate the FLC textile with Ag@ MnO_2-Ppy nanocomposite. In detail; ٥00 mg of CMC was completely dissolved in 30 ml of deionized water under a magnetic stirrer. In this solution, 0.042, and 0.039 M of $KMnO_4$ and $AgNO_3$ oxidants respectively were dissolved accurately. These previous oxidants were impregnated by *FLC* fabric with dimensions of 10*10 cm^2 and then dried at room temperature. This process was repeated several times until the whole mass of oxidant was fully adsorbed on the textile surface. Subsequently, the pyrrole vapor was exposed to a fully dried fabric for 3 h through hanging inside a desiccator to start pyrrole vapor polymerization onto the FLC surface. To the end, the designed fabrics were washed repeatedly with methanol and DIW water to get new ternary composite coated textiles symbolized with AgX-

MODPpy@CMC@FLC where X and D are the added masses from silver nitrate and potassium permanganate powders, respectively. Ag-MOPpy refers to silver and MnO_2 decorated polypyrrole composite, and FLC signifies the bare blend textile. Worthy to note that FLC fabric was individually impregnated with various mass ratios between silver nitrate and potassium permanganate to design new-coated composites of Ag١-MO٢Ppy@FLC, Ag2-MO1Ppy@FLC, AgPpy@FLC, and MOPpy@FLC for comparison purposes.

2.4. Antibacterial activity:

The antimicrobial behavior of treated and untreated Lyocell blend textiles was addressed against (S. aureus) as a Gram-positive bacterium and E. coli as a Gram-negative bacterium by utilizing the agar well diffusion method. In brief, a sterilized solution was prepared by dissolving 10 g tryptone, 5 g yeast extract, and 10 g sodium chloride in 1L of DIW. Thereafter, 5 mL of the former medium was placed in sterilized Petri dishes and left to solidify. Our samples were cut with dimensions of 1*1 cm^2 and then moved to the plates followed by incubation for 24 h at 37 ^oC. After the incubation time, the diameter of inhibition zones for the as-tested samples was measured and the mean value was taken for three reproducible experiments.

2.5. Characterization:

The structural characterization for as-fabricated textiles was investigated using FTIR (Nicolet 380 Thermo Scientific instrument) at a wavenumber range of 4000 to 400 cm^{-1}. The crystal structure of these materials was measured on an X-ray powder diffractometer of a Philips Xpert MPD Pro type with Cu K a (k = 1.5406 Å) radiation, and scan rate of 5 degree/min at 2θ range of 10-80°.

Thermograms for textiles were collected from a thermogravimetric analyzer (TGA-50H Shimadzu) at a temperature range from 30 to 700 °C. A field emission scanning electron

microscope (FE-SEM, Quanta 250 FEG) operated at an accelerating voltage of 30 KV was utilized to check the surface of the coated fabrics.

To study the mechanical features of coated and pure textiles, a tensile testing machine (H1-5KT/S) was utilized where the dimensions of the sample were 15 * 4 cm^2. Furthermore, the electrical resistance of the samples was evaluated with a calibrated digital multimeter (Fluke 8846A) in which all the samples were firstly coated with silver paste. The ultraviolet protection factor (UPF) of treated and untreated fabrics was investigated using a UV–Vis Spectrophotometer with the model of (Shimadzu UV 3101PC).

The flammability evaluation for the developed textiles was done using UL94 by running two tests; first one is a modified standard ISO 3795 [24] where the materials were applied horizontally to a flame height of 38 mm for 15 s. The burning rate (V) in mm/min was estimated based on the following equation:

$$V = \frac{D}{t} \qquad (1)$$

Where D is the burnt distance, and t is the time consumed for burning the material.

The second test is the vertical flame spread test (ASTM D6413) where the fabric specimens were vertically exposed to a flame height of 38 mm and a time of 12 s. The tests were done three times and the average value was taken.

3. Results and discussion:

3.1. Green synthesis route of coated FLC textiles:

A one-pot and eco-friendly approach based on vapor polymerization was developed for coating silver and manganese dioxide @ polypyrrole nanocomposite on FLC textile as seen in Scheme 1. A green binder from O-carboxymethyl chitosan was used for firmly attaching the nanocomposite to the textile for acquiring antibacterial, fire retardancy, conductivity, and UPF features. Using a dipping and drying strategy, the FLC textile was firstly steeped in a freshly prepared solution containing CMC, $KMnO_4$, and $AgNO_3$, and further air-dried. This step was continuously repeated several times until all solutions get adsorbed on the FLC surface. The whole mass of oxidant was fully adsorbed on textile surface.

O-carboxymethyl chitosan contains several function groups that could assist the occurrence of hydrogen and Vander Waals interactions with textile surfaces. Using a vapor polymerization reaction developed in our laboratory, the Ag-MOPpy composite was uniformly formed on the fabrics when pyrrole vapor was exposed to textiles at room temperature. Notably, both $KMnO_4$ and $AgNO_3$ can be acted as effective oxidizing agents to initiate the vapor polymerization of pyrrole monomer [17]. Indeed, condensed vapors are typically noticed at room temperature from a pyrrole bottle which can expedite the polymerization reaction over the surface of various substrates carrying specific oxidizing agents [8, 18-20]. Consequently, $AgNO_3$ and $KMnO_4$ oxidants coated on textile could oxidize pyrrole to polypyrrole polymer and themselves got reduced to form silver and manganese dioxide nanoparticles [21-23]. Observably, the white color of raw FLC textile was altered to brown-black as the first evidence for effective oxidation of pyrrole by both as-used oxidants as presented in Fig. S4.

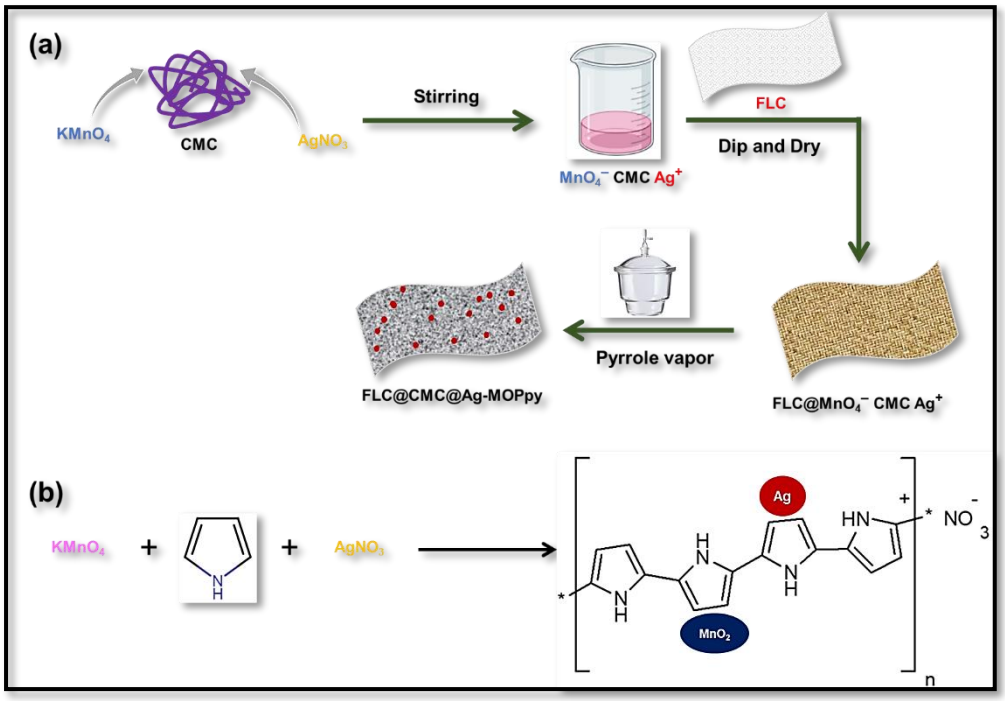

Scheme 1. (a) Schematic diagram for modifying FLC by Ag-MOPpy nanocomposites through facile vapor polymerization approach, and (b) Mechanism of polypyrrole formation using $KMnO_4$, and silver nitrate oxidants.

3.2. Structural elucidation of coated FLC textiles:

The structure of as-formed nanocomposites on FLC textile was chemically elucidated using FTIR spectroscopy, XRD, and TGA. As seen in Fig. 1a, bare blend textile depicts exhibited absorption bands at 3334, 2891, and 1029 cm-1 attributing to the stretching vibration of hydroxyl, CH, and C-O-C groups [24, 25]. When MOPpy nanocomposite was chemically attached to an FLC textile, the FTIR spectrum showed M-O vibrations of α-MnO2 represented by small peaks at 721, and 580 cm-1 [26]. The obvious bands seen at 1428 and 1369 cm-1 are assigned to antisymmetric and symmetric vibrations of the pyrrole ring. The stretching vibration of C=C bonding in the pyrrole ring was characterized by a tiny peak located at 1596 cm-1. In addition, the absorption peak seen at 1315, and 1161 cm-1 were

ascribed to the stretching vibrations of =CH in-plane deformation and C-N group [27, 28]. A characterized band situated at 1161 cm -1 is designated for the stretching of C-N. The charge neutralization of polypyrrole by the dopants or counter ions is proved by the occurrence of an absorption peak at a wavenumber of 1369 cm-1 [8]. Similarly, all the above-described absorption bands were noticed in FLC@Ag-MOPpy, and FLC@CMC@Ag-MOPpy composite with lower intensity and shifting as a result of the incorporation of silver nanoparticles in the MOPpy structure. Moreover, the FTIR curve of FLC@CMC@Ag-MOPpy fabrics assures the structure of CMC by the appearance of absorption bands at 1649, and 1383 elucidating the symmetric and asymmetric stretching (-C=O) group existed in N-acetyl groups.

The crystallographic structure of various coated FLC fabrics was investigated by XRD technique as found in Fig. 1b. A plain sole diffraction peak was noticed in XRD profile of raw FLC fiber at 20.2° attributing the ordered chains of cellulose [29]. However, when the fabric was decorated with MOPpy nanocomposite, a highly crystalline material was acquired where there were characteristic peaks at 2θ equals 12.8°, 27.12°, 28.9°, 36.3°, 38.8°, 40.6°, 42.9°, 46.07°, 47.72°, 50.61°, 55.4°, 62.7°, and 68.92° demonstrating the diffraction planes of (110), (220), (310), (400), (330) (420), (301), (321), (510), (411), (600), (521), and (541) of tetragonal α-MnO2 ((JCPDS: 44-0141) [30]. Additionally, the XRD pattern reveals an apparent peak determined at 21.2° showing the presence of amorphous polypyrrole that was successfully produced by using AgNO3 and KMnO4 as reducing agents for pyrrole monomer [27]. Contrariwise, the crystallinity of MOPpy composite was highly minimized in FLC@CMC@Ag-MOPpy textile when mixed with CMC chains on fabric surface (See Fig. 2b).

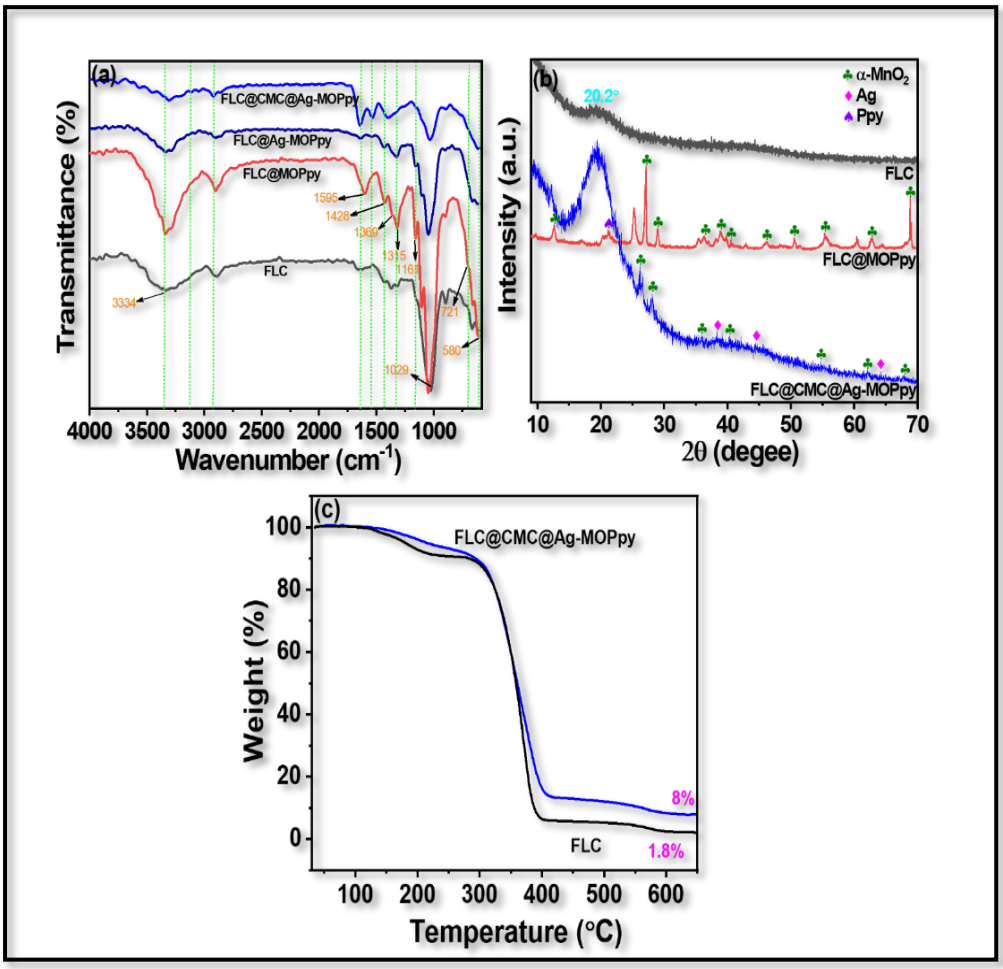

Fig. 2. (a) FTIR spectrums of Raw FLC, FLC@MOPpy, FLC@Ag-MOPpy, and FLC@CMC@Ag-MOPpy fabrics, (b) XRD profiles of bare FLC, FLC@MOPpy, and FLC@CMC@Ag-MOPpy fabrics, and (c) Thermograms of FLC, and FLC@CMC@Ag-MOPpy fabrics.

Besides, the diffraction pattern manifests three peaks that were estimated at 38.2, 44.4, and 64.2° with a small intensity related respectively to (111), (200), and (220) crystalline planes of Ag nanoparticles with references card of JCPDS file No. 004-0783. Such XRD observations can certainly confirm the formation of Ag and MOPpy composite as a smart coating for FLC textile.

The thermal behavior of FLC and its coated FLC@CMC@Ag-MOPpy composite was studied using TGA analysis as seen in Fig. 1c. The thermogram of virgin FLC shows three steps of decomposition; up to 215 °C due to loss of water content, from 230 to 410 °C refers to the essential degradation of function groups found in the cellulose backbone, in addition to small peak observed from 535 °C corresponded to fracture to the carbonic chains giving a rise to a char layer of 1.8% [25, 31]. FLC@CMC@Ag-MOPpy composite composes an identical thermal manner but with delayed decomposition temperatures and higher char yield (8%). The temperature range of the middle decomposition peak for FLC was changed from a range of 230-410 °C to 259-419 °C because of the role of CMC, Ag, MnO2, and polypyrrole. Upon thermal exposure, these components can derive into carbon char containing Ag and MnO2 nanoparticles and in the meantime extensively doped with nitrogen species that are coming from the heat decomposition of CMC and Ppy [8]. This nanocomposite can surely delay the degradation of fabric when exposed to heat.

SEM analysis was carried out for different coatings to get information about their morphology on textile surfaces as seen in Fig. 3. FLC textile in Fig. 3a presents a non-rough morphology without any topography. On the contrary, when the textile was decorated with Ag-MOPpy, it revealed a surface with a remarkable roughness where it is heterogeneously covered with polypyrrole polymer containing manganese dioxide and silver nanospheres as presented in Fig. 3b. Meanwhile, in FLC@CMC@Ag-MOPpy nanocomposite, the textile was homogenously and fully wrapped with MnO_2, and Ag nanoparticles of size diameters of ~583, and 58 nm, respectively grown on Ppy nano granules (See Fig. 3c, d).

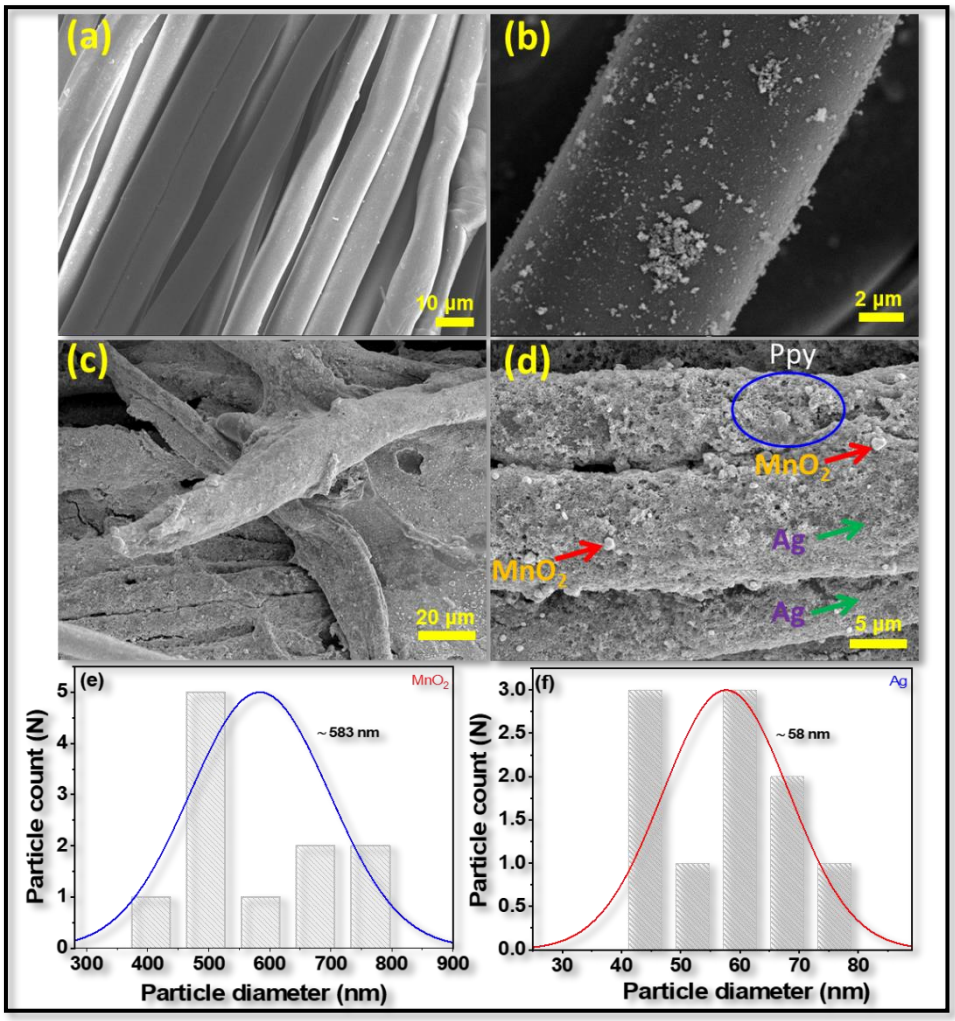

Fig. 3. FE-SEM images of bare FLC (a), FLC@Ag-MOPpy (b), FLC@CMC@Ag-MOPpy at various resolutions (c, d), and particle size distribution of MnO_2, and Ag for FLC@CMC@Ag-MOPpy extracted from their corresponding SEM image (e, f).

The good binding of CMC with textiles plays an important role in improving the particle dispersion in the coating and obtaining a smart porous nanostructure. Such superstructure with highly dispersed Ag-MOPpy composites can ensure multifunctional textiles with antibacterial, flammability, conductivity, and UPF properties. Also, the atomic composition of FLC@CMC@Ag-MOPpy

nanocomposite was accurately analyzed by EDX supplied with SEM as seen in Fig. S5 where it contains C, O, N, Mn, Ag, and K elements confirming the successive formation of silver and MnO_2@ Ppy composite from the oxidation of pyrrole when FLC was coated with $AgNO_3$, and $KMnO_4$ as reducing agent and exposed to its vapor at ambient conditions.

3.3. Mechanical properties, Electrical conductivity, UPF of FLC coatings:

When Ag-MOPpy composites were utilized as coatings for textiles, the mechanical properties were expected to change, thus parameters like elongation (G) and tensile strength (T) of untreated and treated textiles were estimated and tabulated in Table 1. The data stated that FLC textile offered G, and T values of 8.58%, and 701 N, respectively. However, when Ag-MOPpy was loaded on textile surface, considerable damage to the mechanical properties was noticed. This effect was highly observed when the mass ratios between $AgNO_3$ and $KMnO_4$ were gradually minimized. The FLC@Ag2-MO1Ppy coating could decrease the G, and T values of FLC textile to 6.18%, and 268 N, respectively which are lower than the blank coatings of FLC@MOPpy (8.41%, 355 N) and FLC@AgPpy (8.84%, 350 N). The bad dispersion of both silver and MnO_2 nanoparticles in the coating structure can allow their entry inside the structure of the fiber and hence can highly affect the mechanical properties [17]. This behavior was diminished when the textile was coated with polypyrrole composite containing one type of nanoparticle. Nevertheless, when CMC was used as in the coating layer, it could guarantee a better dispersion of polypyrrole-based composites with silver and MnO_2 nanoparticles on the textile surface as in FLC@CMC@Ag-MOPpy preventing their potential to enter into the textile chains, and thus resulting in a remarkable improving in the mechanical features of FLC textile. Interestingly, this fabric could realize a higher T value of 563.3 N, which is close to that of pure FLC.

Over and above, G was substantially recorded as 12.3% which is superior with respect to the bare FLC (8.58%) demonstrating that FLC@CMC@Ag-MOPpy coating could enhance the elastic behavior of blend FLC textile. This might be owing to the incident hydrogen binding that happened between CMC and Ag-MOPpy with the hydroxyl groups of textiles. This force can not only assist the stress transfer from the textile structure to the coating but also fastens the polymer crystallization [32].

Table 1. Mechanical features of FLC and its various prepared coatings.

Sample code	Tensile stress [N]	Elongation [%]
FLC	701	8.58
FLC@Ag-MOPpy	470.5	8.07
FLC@Ag2-MO1Ppy	201	6.15
FLC@Ag1-MO2Ppy	268	6.18
FLC@MOPpy	355	8.41
FLC@AgPpy	350	8.84
FLC@CMC@Ag-MOPpy	563.3	12.3

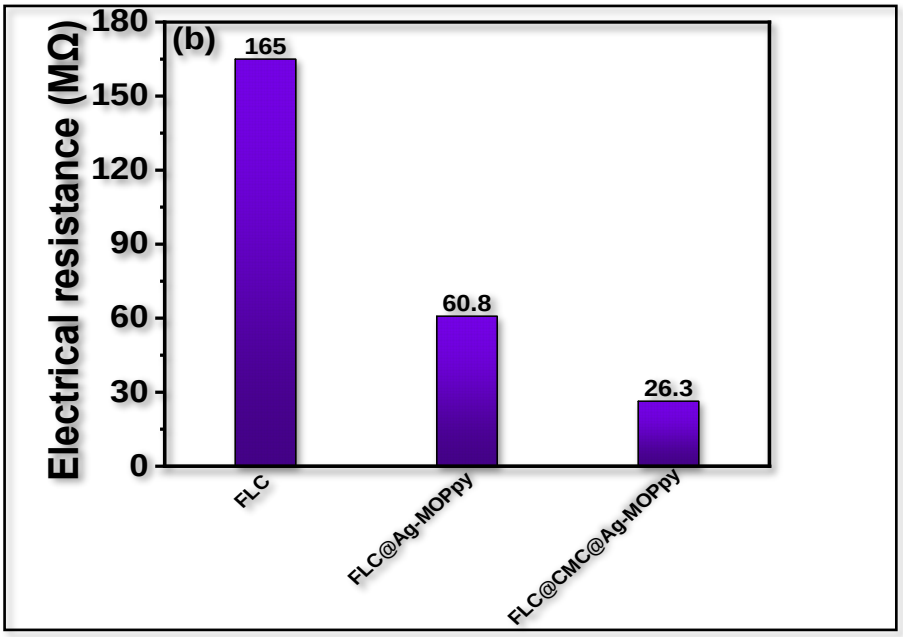

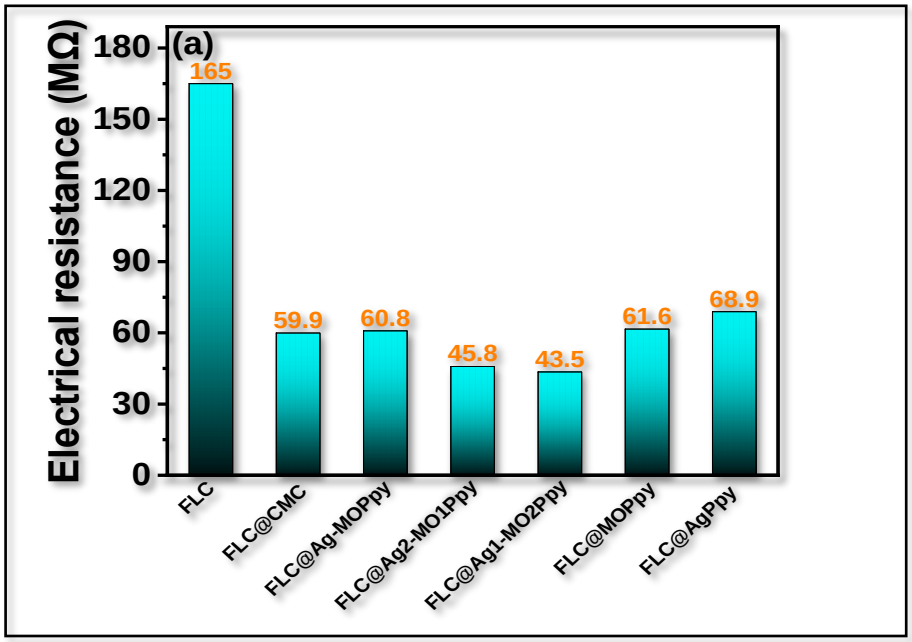

Fig. 4. Electrical resistance of FLC, FLC@CMC, FLC@Ag-MOPpy, FLC@Ag2-MO1Ppy, FLC@Ag1-MO2Ppy, FLC@MOPpy, FLC@AgPpy (a), Comparison in resistance between FLC, FLC@Ag-MOPpy, and FLC@CMC@Ag-MOPpy coatings (b).

The electrical conductivity of blend FLC fabric and its developed coatings was expressed by measuring the resistance as drawn in Fig. 4. The results confirm the non-conductivity of pure FLC as it achieves a resistance value of 165 MΩ. Whereas, the modification of FLC with CMC compound causes a sudden decrease in electrical conductivity to 59.9 MΩ because the incorporation of the carboxymethyl group to chitosan chains can improve ionic conductivity by the free movements of ions and segments [33]. As seen in Fig. 4a, the pyrrole polymerization on FLC by using KMnO4 and $AgNO_3$ oxidants with a mass ratio 2:1 results in strikingly minimizing the resistance to 43.5 MΩ as in FLC@Ag1MO2Ppy sample which is relatively lower than the blanks of FLC@AgPpy (61.6 MΩ), and FLC@MOPpy (68.9 MΩ). This is due to the conductive properties of polypyrrole, MnO_2, and Ag nanomaterials that existed in the coating [34, 35]. The further raising of mass ratio between $KMnO_4$ and $AgNO_3$ oxidants leads to a

gradual increase of resistance and hence minifying the conductivity of final textile (See Fig. 4a). Interestingly, the FLC@CMC@Ag-MOPpy fabric could attain an inferior resistance value of 26.3 MΩ when compared with the virgin FLC (165 MΩ), and FLC@Ag-MOPpy (165 MΩ) characterizing high conductive substrate as expressed in Fig. 4b. This behavior highlights an effective synergism occurring between CMC and Ag-MOPpy where the utilization of CMC in the coating as a binder could secure an outstanding dispersion for silver and MnO_2@Ppy composite and consequently achieve an enhancement in the electrical conductivity of textile.

Due to their organic nature, the exposure of textiles to UV radiation can stimulate their damage and hence cause many diseases to human [36, 37]. Consequently, it is important to adhere a UV protection property by coating textiles with nanomaterials that could absorb UV rays to extend the application of textiles. In general, paramount information about the absorbance and transmittance of UV light on fabric surface can be provided by measuring the Ultraviolet Protection factor (UPF). Substrates with higher UPF values assigns for low UV transmittance and high protection ability against UV radiation. UPF of FLC, FLC@Ag-MOPpy, and FLC@CMC@Ag-MOPpy samples was measured and the data was summarized in Fig. 5. UPF for pure FLC was recorded as 6.2 demonstrating a highly sensitive material to UV radiation. However, the UV absorption of the textile was greatly improved when coated with Ag-MOPpy composite as it attained an UPF value of 20.5, which is about 3.3 times that observed for the raw FLC because Ag, MnO_2, and Ppy can absorb UV rays. More considerably, FLC@CMC@Ag-MOPpy depicts the highest UPF value (33.69) which is 5.4 folds in comparison with pure FLC presenting effective synergism CMC and Ag-MOPpy composite in the UV protection ability [38, 39].

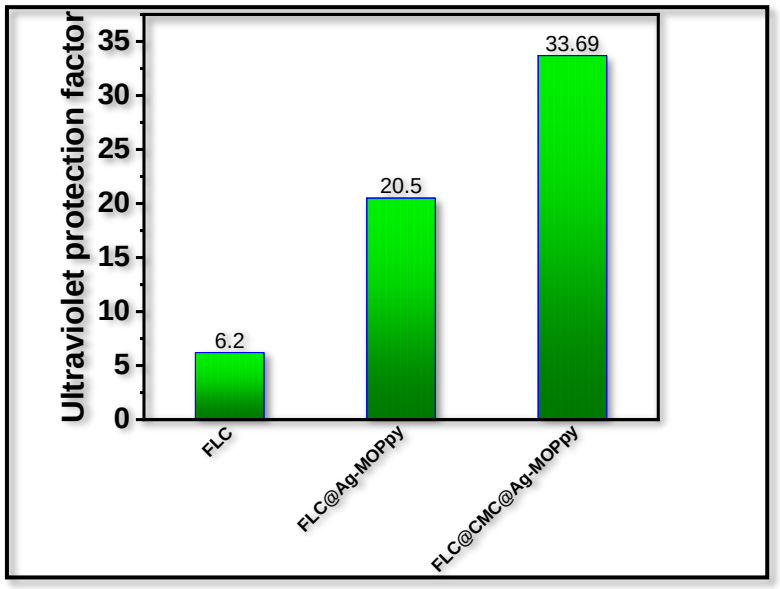

Fig. 5. UPF comparison between FLC, FLC@Ag-MOPpy, and FLC@CMC@Ag-MOPpy coatings.

3.4. Antibacterial performance, and fire retardancy of FLC coatings:

Additionally, the bacterial behavior of various treated textiles was evaluated by performing agar diffusion test where the diameter of inhibition zones was estimated after the material was incubated in agar petri dishes for 24 h as displayed in Fig. 6, Table 2. The unmodified FLC fabric shows no inhibition for E. coli and S. aureus bacteria. However, when CMC, MOPpy, and AgPpy were individually coated on pure textile, the bacterial inhibition diameter was recorded in sequence as 15, 16, and 19 mm for E. coli and 0, 17, and 18 mm for S. aureus confirming the antibacterial activity of carboxymethyl chitosan, silver, and manganese dioxide. The dual formation of AgNPs and MnO2 with polypyrrole on the FLC surface as in FLC@Ag2-MO1Ppy increases inhibition diameter to 19 and 20 mm for E. coli, and S. aureus, respectively. Notably, the variation in mass ratio between AgNO3 and $KMnO_4$ when preparing polypyrrole on textile surfaces such as FLC@Ag1-MO2Ppy, and FLC@Ag-MOPpy

depicts no significant change in bacterial retardation. Meanwhile, It was inspired when CMC was used as a better dispersant for AgNPs and MnO_2 as a coating for FLC textile, the antimicrobial efficiency was substantially improved as it accomplished inhibition diameter of 29, and 28 mm for E. coli, and S. aureus, respectively compared to FLC@Ag-MOPpy blank (18, 17 mm) assuring an excellent synergism occurred between CMC and Ag-MOPpy. Such composite can effectively retard bacterial growth because the probable interaction of carboxylic groups with amino groups on the CMC surface can produce a highly positively charged polymer, which can easily interact with the negatively charged wall of bacteria. Additionally, MnO_2 nanospheres can generate highly energetic species such as OH^-, H_2O_2, and $O2^{2+}$ where hydrogen peroxide can easily penetrate through the cell, besides OH^- and $O2^{2+}$ can destroy the cell membrane and wall [40, 41].

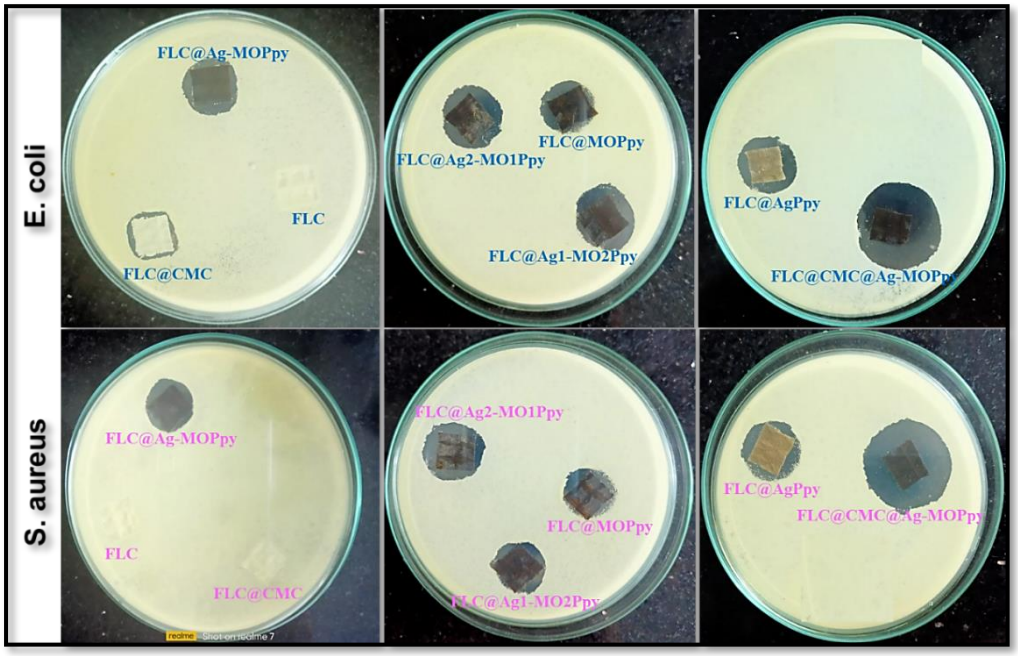

Fig. 6. Antimicrobial behaviors of FLC, FLC@CMC, FLC@Ag-MOPpy, FLC@Ag2-MO1Ppy, FLC@Ag1-MO2Ppy, FLC@MOPpy, FLC@AgPpy, FLC@CMC@Ag-MOPpy coatings against E. coli, and S. aureus bacteria.

Table 2. Bacterial inhibition diameters calculated for FLC and its nanocomposite coatings.

Sample code	Inhibition zone(mm)	
	E. coli	S. aureus
FLC	0	0
FLC@CMC	15	0
FLC@Ag-MOPpy	18	17
FLC@Ag2-MO1Ppy	19	20
FLC@Ag1-MO2Ppy	18	19
FLC@MOPpy	16	17
FLC@AgPpy	19	18
FLC@CMC@Ag-MOPpy	29	28

Table 3. The horizontal burning rate measured for uncoated and coated FLC blended samples.

Sample code	Rate of Burning [mm/min]	Observations
FLC	172.5	The flame passed the second mark
FLC@CMC	144	The flame passed the second mark
FLC@Ag-MOPpy	0	The glowing passed the second mark
FLC@CMC@Ag-MOPpy	0	The glowing passed the second mark

Table 4. Vertical flammability data estimated for uncoated and coated FLC blended samples.

Sample code	Afterflame time [s]	Afterglow time [s]	Char length [mm]
FLC	14	35	300
FLC@CMC	17	55	300
FLC@Ag-MOPpy	0	270	150
FLC@CMC@Ag-MOPpy	0	395	100

UL94 flame chamber was exploited to study the fire safety of as-coated FLC textiles by applying two standard test methods; ISO standard 3795 (Horizontal flame spreading test), and ASTM D6413 (Vertical flame test), and the data were tabulated in Tables 3 and 4. When the flame source ignited a pure FLC textile, it was fully burned with a rate of burning of 172.5 mm/min because of its carbonic nature. Whereas, the coating of CMC on the FLC surface causes a decrease in rate of burning to 144 mm/min approving the retardation of flame growth. Remarkably, the coating containing Ag-MOPpy can stop the flame progress on FLC as a result of forming a compact and protective layer from AgNPs, MnO_2, and nitrogen-doped carbon char that can restrict the flammable volatiles convection to the flame zone [42]. Moreover, the ternary composite of FLC@CMC@Ag-MOPpy pictured the same rate of burning value assuring an improved flame retardancy performance of our textiles.

In a different way, the upward flammability of as-developed fabrics was investigated by running a vertical flame test according to ASTM D6413 where essential parameters like afterflame and afterglow times, and char length were measured (See Table 3). The data stated that FLC blank was completely fired with estimated afterflame and afterglow times of 14, and 35 s, consecutively with no observable char. On the contrary, the flammability behavior of FLC was improved when dipped in CMC polymer where it achieves afterflame and afterglow times of 17, and 55 s with a recorded char length of 300 mm. Interestingly, FLC@CMC@Ag-MOPpy, and FLC@Ag-MOPpy composites presents a highly improved fire retardancy because their combustion was instantly ended showing no afterflame time. Besides, their afterglow times were noted as 395, 270 s, respectively which are relatively longer compared to the unmodified FLC (35 s), and FLC@CMC (55 s) and were found to meet the ASTM D6413-99 standard. It is pertinent to know that FLC@CMC@Ag-MOPpy plains the lowest burnt char length among all fabricated

textiles where it was measured as 100 mm. It can be concluded that the facile vapor polymerization of pyrrole succeeded in obtaining multifunctional textiles with outstanding flame retardancy, UPF, antibacterial, and conductivity which can be applied in advanced fields.

Conclusion:

The in-situ formation of Ag-MOPpy composite on Lyocell-based fabrics was executed using a green and easy PVP approach with the assistance of $AgNO_3$, and $KMnO_4$. CMC polymer was used to ensure the uniform dispersion of silver and manganese dioxide@Polypyrrole in the coating layer for obtaining smart multifunctional textiles. Notably, MnO_2 and Ag nanoparticles were grown inside polypyrrole nano granules on textile with size diameters of ~583, and 58 nm, respectively. Adding to this, the UV protection, conductivity, antimicrobial activity, and fire safety properties were studied. The electrical resistance of the composite modified textiles was estimated as 26.3 MΩ, which is relatively lower than the pure Lyocell fabric (165 MΩ) as an indication for high conductive material. A highly improved ultraviolet protection factor was also recorded for the coated textile (33.69) compared to the pure one (6.2). The textile composites could retard the microbial infection with a measured inhibition zone diameter of 29, and 28 mm for E. coli, and S. aureus, respectively approving an excellent antimicrobial manner. Moreover, the flammability tests stated that the rate of burning for as-coated textile was measured as 0 mm/min with regard to the virgin Lyocell fabric (172.5 mm/min). In addition, the afterflame, and glow times were noted as 0 sec, and 395 s compared to 14, and 35 sec for the uncoated textiles assuring an efficient retardation performance against flame spread.

References:

[1] Q.-y. Zhang, X.-h. Liu, Y.-l. Ren, Y.-g. Zhang, B.-w. Cheng, Fabrication of a high phosphorus–nitrogen content modifier with star structure for effectively enhancing flame retardancy of lyocell fibers, Cellulose, 27 (2020) 8369-8383.
[2] F. Zhang, Y. Lu, C. Wan, P. Tian, M. Liu, G. Zhang, A bio-resourced mannitol phospholipid ammonium reactive flame retardant for cotton with efficient antiflaming and durability, Cellulose, 27 (2020) 4803-4815.
[3] K.J. Edgar, H. Zhang, Antibacterial modification of Lyocell fiber: A review, Carbohydrate polymers, 250 (2020) 116932.
[4] K. Xie, A. Gao, Y. Zhang, Flame retardant finishing of cotton fabric based on synergistic compounds containing boron and nitrogen, Carbohydrate polymers, 98 (2013) 706-710.
[5] S.T. Dubas, P. Kumlangdudsana, P. Potiyaraj, Layer-by-layer deposition of antimicrobial silver nanoparticles on textile fibers, Colloids and Surfaces A: Physicochemical and Engineering Aspects, 289 (2006) 105-109.
[6] D. Kesavapillai Sreedeviamma, A. Remadevi, C.V. Sruthi, S. Pillai, S. Kuzhichalil Peethambharan, Nickel electrodeposited textiles as wearable radar invisible fabrics, Journal of Industrial and Engineering Chemistry, 88 (2020) 196-206.
[7] Y. Ding, W. Xu, W. Wang, H. Fong, Z. Zhu, Scalable and Facile Preparation of Highly Stretchable Electrospun PEDOT:PSS@PU Fibrous Nonwovens toward Wearable Conductive Textile Applications, ACS Applied Materials & Interfaces, 9 (2017) 30014-30023.
[8] E.S. Goda, M.H. Abu Elella, S.E. Hong, B. Pandit, K.R. Yoon, H. Gamal, Smart flame retardant coating containing carboxymethyl chitosan nanoparticles decorated graphene for obtaining multifunctional textiles, Cellulose, 28 (2021) 5087-5105.

[9] C.-H. Xue, J. Chen, W. Yin, S.-T. Jia, J.-Z. Ma, Superhydrophobic conductive textiles with antibacterial property by coating fibers with silver nanoparticles, Applied Surface Science, 258 (2012) 2468-2472.
[10] X. Jiang, X. Tian, J. Gu, D. Huang, Y. Yang, Cotton fabric coated with nano TiO2-acrylate copolymer for photocatalytic self-cleaning by in-situ suspension polymerization, Applied Surface Science, 257 (2011) 8451-8456.
[11] P.J. Davies, A.R. Horrocks, A. Alderson, The sensitisation of thermal decomposition of ammonium polyphosphate by selected metal ions and their potential for improved cotton fabric flame retardancy, Polymer Degradation and Stability, 88 (2005) 114-122.
[12] Y. Wang, X. Li, Y. Wang, Y. Liu, Y. Bai, R. Liu, G. Yuan, High-performance flexible MnO2@carbonized cotton textile electrodes for enlarged operating potential window symmetrical supercapacitors, Electrochimica Acta, 299 (2019) 12-18.
[13] M. Tian, M. Du, L. Qu, K. Zhang, H. Li, S. Zhu, D. Liu, Conductive reduced graphene oxide/MnO2 carbonized cotton fabrics with enhanced electro -chemical, -heating, and -mechanical properties, Journal of Power Sources, 326 (2016) 428-437.
[14] P. Bober, J. Liu, K.S. Mikkonen, P. Ihalainen, M. Pesonen, C. Plumed-Ferrer, A. von Wright, T. Lindfors, C. Xu, R.-M. Latonen, Biocomposites of Nanofibrillated Cellulose, Polypyrrole, and Silver Nanoparticles with Electroconductive and Antimicrobial Properties, Biomacromolecules, 15 (2014) 3655-3663.
[15] Y.-C. Liu, Sandwiched structure of Ag/polypyrrole/Au to improve the surfaced-enhanced Raman scattering, Electrochemistry Communications, 7 (2005) 1071-1076.
[16] Y.-C. Liu, S.-J. Yang, New pathway for the synthesis of gold and silver bimetallic nanocomplexes and their derivatives of polypyrrole nanorods (TM04096), Electrochimica Acta, 50 (2005) 3674-3678.

[17] M.H. Abu Elella, E.S. Goda, K.R. Yoon, S.E. Hong, M.S. Morsy, R.A. Sadak, H. Gamal, Novel vapor polymerization for integrating flame retardant textile with multifunctional properties, Composites Communications, 24 (2021) 100614.
[18] Z. Hanif, D. Shin, D. Choi, S.J. Park, Development of a vapor phase polymerization method using a wet-on-wet process to coat polypyrrole on never-dried nanocellulose crystals for fabrication of compression strain sensor, Chemical Engineering Journal, 381 (2020) 122700.
[19] X. Zhou, Z. Zhang, X. Xu, X. Men, X. Zhu, Facile Fabrication of Superhydrophobic Sponge with Selective Absorption and Collection of Oil from Water, Industrial & Engineering Chemistry Research, 52 (2013) 9411-9416.
[20] D.O.S. Ramirez, A. Varesano, R.A. Carletto, C. Vineis, I. Perelshtein, M. Natan, N. Perkas, E. Banin, A. Gedanken, Antibacterial properties of polypyrrole-treated fabrics by ultrasound deposition, Materials Science and Engineering: C, 102 (2019) 164-170.
[21] Y.V. Korshak, M.V. Motyakin, I.V. Plyushchii, A.L. Kovarskii, Y.N. Degtyarev, A.G. Petrushevska, R.A. Alekperov, V.A. Dyatlov, A.M. Tsatsakis, A.L. Luss, Y.O. Mezhuev, Pyrrole oxidative polymerization by manganese oxide (IV) on silica gel surface, Polymer, 180 (2019) 121717.
[22] S. Reisi, H. Farimaniraad, M. Baghdadi, M.A. Abdoli, Immobilization of polypyrrole on waste face masks using a novel in-situ-surface polymerization method: removal of Cr(VI) from electroplating wastewater, Environmental Technology, (2023) 1-12.
[23] S.R. Ede, S. Anantharaj, U. Nithiyanantham, S. Kundu, DNA-encapsulated chain and wire-like β-MnO2 organosol for oxidative polymerization of pyrrole to polypyrrole, Physical Chemistry Chemical Physics, 17 (2015) 5474-5484.

[24] Q. Zhang, J. Chen, D. Li, L. Sun, Y. Ren, C. Cheng, X. Liu, Simultaneous enhancement of mechanical strength and flame retardancy of lyocell fiber via filling fire-resistant cellulose-based derivative, Industrial Crops and Products, 199 (2023) 116757.
[25] N. Mengal, I.A. Sahito, A.A. Arbab, K.C. Sun, M.B. Qadir, A.A. Memon, S.H. Jeong, Fabrication of a flexible and conductive lyocell fabric decorated with graphene nanosheets as a stable electrode material, Carbohydrate Polymers, 152 (2016) 19-25.
[26] W. Yao, H. Zhou, Y. Lu, Synthesis and property of novel MnO2@polypyrrole coaxial nanotubes as electrode material for supercapacitors, Journal of Power Sources, 241 (2013) 359-366.
[27] J. Li, L. Cui, X. Zhang, Preparation and electrochemistry of one-dimensional nanostructured MnO2/PPy composite for electrochemical capacitor, Applied Surface Science, 256 (2010) 4339-4343.
[28] S. Shivakumara, N. Munichandraiah, In-situ preparation of nanostructured α-MnO2/polypyrrole hybrid composite electrode materials for high performance supercapacitor, Journal of Alloys and Compounds, 787 (2019) 1044-1050.
[29] J.K. Bediako, W. Wei, S. Kim, Y.-S. Yun, Removal of heavy metals from aqueous phases using chemically modified waste Lyocell fiber, Journal of Hazardous Materials, 299 (2015) 550-561.
[30] S. Ramesh, H.M. Yadav, K. Karuppasamy, D. Vikraman, H.-S. Kim, J.-H. Kim, H.S. Kim, Fabrication of manganese oxide@nitrogen doped graphene oxide/polypyrrole (MnO2@NGO/PPy) hybrid composite electrodes for energy storage devices, Journal of Materials Research and Technology, 8 (2019) 4227-4238.
[31] Y. Guo, M. Xiao, Y. Ren, Y. Liu, Y. Wang, X. Guo, X. Liu, Synthesis of an effective halogen-free flame retardant rich in phosphorus and nitrogen for lyocell fabric, Cellulose, 28 (2021) 7355-7372.

[32] E.S. Goda, B.S. Singu, S.E. Hong, K.R. Yoon, Good dispersion of poly (δ-gluconolactone)-grafted graphene in poly (vinyl alcohol) for significantly enhanced mechanical strength, Materials Chemistry and Physics, 254 (2020) 123465.
[33] N.N. Mobarak, A. Ahmad, M.P. Abdullah, N. Ramli, M.Y.A. Rahman, Conductivity enhancement via chemical modification of chitosan based green polymer electrolyte, Electrochimica Acta, 92 (2013) 161-167.
[34] B.S. Singu, E.S. Goda, K.R. Yoon, Carbon Nanotube–Manganese oxide nanorods hybrid composites for high-performance supercapacitor materials, Journal of Industrial and Engineering Chemistry, 97 (2021) 239-249.
[35] B.S. Singu, K.R. Yoon, Highly exfoliated GO-PPy-Ag ternary nanocomposite for electrochemical supercapacitor, Electrochimica Acta, 268 (2018) 304-315.
[36] A. Bashari, M. Shakeri, A.R. Shirvan, 12 -UV-protective textiles, in: I. Shahid ul, B.S. Butola (Eds.) The Impact and Prospects of Green Chemistry for Textile Technology, Woodhead Publishing, 2019, pp. 327-365.
[37] S. Mondal, Nanomaterials for UV protective textiles, Journal of Industrial Textiles, 51 (2021) 5592S-5621S.
[38] M. Hasani, M. Mahdavian, H. Yari, B. Ramezanzadeh, Versatile protection of exterior coatings by the aid of graphene oxide nano-sheets; comparison with conventional UV absorbers, Progress in Organic Coatings, 116 (2018) 90-101.
[39] X. Chen, N. Yu, L. Zhang, Z. Liu, Z. Wang, Z. Chen, Synthesis of polypyrrole nanoparticles for constructing full-polymer UV/NIR-shielding film, RSC Advances, 5 (2015) 96888-96895.
[40] F. Wahid, J.-J. Yin, D.-D. Xue, H. Xue, Y.-S. Lu, C. Zhong, L.-Q. Chu, Synthesis and characterization of antibacterial carboxymethyl Chitosan/ZnO nanocomposite hydrogels, International Journal of Biological Macromolecules, 88 (2016) 273-279.

[41] E. Cherian, A. Rajan, G. Baskar, Synthesis of manganese dioxide nanoparticles using co-precipitation method and its antimicrobial activity, International Journal of Modern Science and Technology, 1 (2016) 17-22.
[42] E.S. Goda, M.H. Abu Elella, H. Gamal, S.E. Hong, K.R. Yoon, Two-Dimensional Nanomaterials as Smart Flame Retardants for Polyurethane, in: Materials and Chemistry of Flame-Retardant Polyurethanes Volume 1: A Fundamental Approach, American Chemical Society, 2021, pp. 189-219.